

KeV dark matter in minimal extended seesaw model and its predictions in neutrinoless double beta decay and baryogenesis.

Mayengbam Kishan Singh,^{1,*} S. Robertson Singh,^{2,3,†} and N. Nimai Singh^{2,3,‡}

¹*Department of Physics, Manipur University, Imphal-795003, India*

²*Department of Physics, Manipur University, Imphal - 795003, India*

³*Research Institute of Science and Technology, Imphal - 795003, India*

Abstract

We develop an $A_4 \times Z_4 \times Z_2$ symmetry extension of Standard Model under the minimal extended seesaw (MES) mechanism which successfully predicts neutrino masses and mixings patterns. This model breaks $\mu - \tau$ symmetry of neutrino mass matrix and explains leptonic mixing with non-zero θ_{13} . We study the phenomenological results of the keV-scale sterile neutrino as a dark matter candidate along with other phenomenologies such as neutrino oscillation observables, neutrinoless double beta decay, baryogenesis via leptogenesis, etc. Dirac CP-violating phase δ_{CP} and two Majorana phases α and β are also calculated from the leptonic mixing matrix. Best-fit values of the model parameters and neutrino observables are calculated from χ^2 analysis. The model predicts best-fit values of neutrino mixing angles to be $\sin^2 \theta_{23} = 0.555$, $\sin^2 \theta_{12} = 0.301$ and $\sin^2 \theta_{13} = 0.022$ for normal hierarchy. Significant results consistent with experimental data are also observed for effective neutrino mass $m_{\beta\beta} \sim (0.97 - 5.02)$ meV, effective electron mass $m_\beta \sim (0.084 - 0.41)$ eV and sum of active neutrino masses $\sum m_i < 0.12$ eV. The model does not favour Inverted hierarchy at the 3σ level with the given parameter space.

* kishan@manipuruniv.ac.in

† robsoram@gmail.com

‡ nimai03@yahoo.com

I. INTRODUCTION

Inspite of enormous successes and outstanding discovery of Higg's boson, the Standard Model (SM) is incapable of explaining many problems and phenomena in the Universe. Absence of neutrino mass is one of the main shortcomings of SM. Observations of neutrino oscillation in SNO[1, 2], SK[3], etc. have verified that neutrinos have non-zero mass and they can change from one flavour to another. The global analysis of the latest data from various experiments such as solar, atmospheric, reactor and accelerator experiments, gives the best fit values of the neutrino oscillation parameters such as the two mass-squared differences ($\Delta m_{atm}^2 \sim 7.4 \times 10^{-5} \text{eV}^2$ and $\Delta m_{sol}^2 \sim 2.5 \times 10^{-3} \text{eV}^2$) and the three mixing angles ($\theta_{12} \sim 34^\circ$, $\theta_{13} \sim 7.4^\circ$ and $\theta_{23} \sim 48^\circ$)[4]. Some of the burning questions in high energy physics are the absolute masses and exact nature of the neutrinos (Dirac or Majorana), Dirac CP-violating phase, baryon asymmetry of the Universe (BAU), dark matter (DM), etc.

Anomalies in the observations of LSND[5] which detected an excess of electron anti-neutrino ($\bar{\nu}_e$) in a muon anti-neutrino ($\bar{\nu}_\mu$) beam produced at the Los Alamos laboratory could not be explained by the three neutrino oscillation scheme. This result was further supplemented by the MiniBooNE [6] experiment which observed an oscillation from ($\bar{\nu}_\mu$) to ($\bar{\nu}_e$) in agreement with the LSND data. These observations gave birth to the idea of the existence of additional neutrino(s) called sterile neutrino. Sterile neutrinos are singlet fermions under $SU(2)_L$ which do not have weak interactions but can mix with the active neutrinos. LSND and MiniBooNE results could be explained by adding at least one additional sterile neutrino having mass in the eV scale to the SM in a $3 + 1$ framework. However, sterile neutrino with different mass scales can play important role in many cosmological phenomena. Recent results from MicroBooNE suggests the non-possibility for existence of an eV scale sterile neutrino. But, keV to GeV scale sterile neutrinos are still well-motivated theoretically and do not contradict any existing experiments[7].

Cosmological and astrophysical measurements have indicated the presence of a mysterious, non-luminous, non-baryonic matter called dark matter(DM) which accounts for 26.8% of the total energy density of the Universe [9, 10]. Yet, the fundamental nature of DM i.e. their origin, its constituents and interactions are still unknown. The requirements of a DM particle [11] rule out all the SM particles. One of the most interesting beyond Standard

parameter	best fit $\pm 1\sigma$	3σ range
$ \Delta m_{21}^2 : [10^{-5}eV^2]$	$7.41^{+0.21}_{-0.20}$	6.82–8.03
$ \Delta m_{31}^2 : [10^{-3}eV^2](NO)$	$2.511^{+0.028}_{-0.027}$	2.428–2.597
$ \Delta m_{32}^2 : [10^{-3}eV^2](IO)$	$2.498^{+0.032}_{-0.025}$	2.408–2.581
$\sin^2 \theta_{12}$	$0.303^{+0.012}_{-0.011}$	0.270–0.341
$\sin^2 \theta_{23}(NO)$	$0.572^{+0.018}_{-0.023}$	0.406–0.620
$\sin^2 \theta_{23}(IO)$	$0.578^{+0.016}_{-0.021}$	0.412–0.623
$\sin^2 \theta_{13}(NO)$	$0.02203^{+0.00056}_{-0.00059}$	0.02029–0.02391
$\sin^2 \theta_{13}(IO)$	$0.02219^{+0.00060}_{-0.00057}$	0.02047–0.02396
$\delta_{CP}/^\circ(NO)$	$197^{+42}_{-0.25}$	108–404
$\delta_{CP}/^\circ(IO)$	286^{+27}_{-32}	192–360

TABLE I. Updated global-fit data for three neutrino oscillation, *NuFit 2022*[8].

Model(BSM) particle which behave as a warm dark matter (WDM) is the sterile neutrino. Particularly, sterile neutrinos with masses in the keV range having very small mixing with the active neutrinos of the order of $\sin^2 2\theta \sim \mathcal{O}(10^{-10})$ can be a dark matter [12–14]. According to the latest Planck data [15], the relative abundance of DM in the Universe is observed as

$$\Omega_{DM}h^2 = 0.1187 \pm 0.0017 \quad (1)$$

Dodelson-Widrow mechanism[16] provides the correct abundance of keV-scale sterile neutrinos as DM. It requires only the mixing between active and heavier sterile neutrino, and thus this mechanism is very well-motivated. Further, the Shi-Fuller mechanism[17] which includes lepton asymmetries, can result in resonantly enhanced production of sterile neutrinos. This allows it to access a larger range of the $m_s - \theta_s$ parameter space. The stability of keV sterile neutrino at the cosmological scale is one of the most important criteria to

be a DM candidate. Sterile neutrinos can radiatively decay into an active neutrino and a monoenergetic photon through $\nu_s \rightarrow \nu_a + \gamma$. The decay rate is given by [18, 19]

$$\Gamma = 1.38 \times 10^{-32} \left(\frac{\sin^2 2\theta}{10^{-10}} \right) \left(\frac{m_s}{keV} \right)^5 s^{-1} \quad (2)$$

where $\sin^2 2\theta = 4 \sum_i^{e,\mu,\tau} |U_{i4}|^2$ is the effective active-sterile mixing angle and $|U_{i4}|$ are the elements of active-sterile mixing matrix. The sterile neutrino lifetime is thus sufficiently large and it is essentially stable over timescales comparable to the age of the Universe $t_U = 4.4 \times 10^{17} \text{sec}$ [15], so that it is a good DM candidate. Following Ref.[20?], the sterile neutrino abundance is expressed as a function of active-sterile mixing angle θ and the mass of sterile neutrino m_s as

$$\Omega_{DM} h^2 \simeq 0.3 \left(\frac{\sin^2 2\theta}{10^{-10}} \right) \left(\frac{m_s}{100keV} \right)^2 \quad (3)$$

There are constraints on the mass and mixing of the keV-scale sterile neutrino with active neutrinos provided by various cosmological and laboratory experiments such as observed DM relic density[21], X-ray searches for sterile neutrino decay[22–26], Lyman- α forests[27], Tremaine-Gunn[28] and phase-space analysis[29], etc. Combining these constraints, we can infer that the mass of the sterile neutrino should be $m_s \geq 4 \text{ keV}$, and its mixing with SM neutrinos should be $\sin^2 2\theta \leq 10^{-6}$ [30]. Various works on neutrino models based on the study of keV-mass sterile neutrinos as DM can be found in Refs.[20, 31–35]. Detailed analysis on the production and decay of keV-scale sterile neutrino DM in the early Universe are given in Refs.[32, 36–39]. Searches for decaying DM signal in the keV-MeV mass range have been conducted using a wide range of X-ray telescope, XMM-Newton[40–42], Chandra[43–45], Suzaku[46, 47], Swift[48], NuStar[49–51] etc. There also has been an unknown observation of a 3.5 keV line in the X-ray spectra of galaxy clusters[52] as well as Andromeda[53] and Milky Way galaxies[54]. This could be interpreted as a signal coming from the decay of DM particle having mass $\sim 7 \text{ keV}$ [55]. However, this result is widely disputed and future progress with our understanding of the origin and nature of this signal may come with the next generation of high-resolution X-ray missions, including XARM (Hitomi replacement mission), LYNX and Athena+[56].

Another important problem that we shall address here is the origin of matter-antimatter asymmetry of the Universe. The current data on this Baryon Asymmetry of Universe (BAU) is given by

$$Y_B = \frac{\eta_B - \eta_{\bar{B}}}{s} \simeq (8.7 \pm 0.06) \times 10^{-11} \quad (4)$$

Fukugida and Yanagida[57, 58] showed that if heavy right-handed Majorana neutrinos exist, they can decay in a lepton number violating process to the SM leptons and Higgs boson. If C and CP are violated in these decays, there can be symmetry between leptons and anti-leptons. Finally, the lepton asymmetry is converted into baryon asymmetry through sphaleron process and thus producing matter-antimatter asymmetry. Many authors have discussed baryogenesis via leptogenesis in different neutrino models[34, 59–62].

Further, neutrinoless double beta decay ($0\nu\beta\beta$) is also one of the most important experiments to probe the Dirac or Majorana nature of neutrinos[63, 64]. These experiments are also sensitive to the absolute neutrino masses through the effective neutrino mass $m_{\beta\beta}$. KAMLand-Zen[65] and GERDA provided an upper bound on $m_{\beta\beta}$ through a combined analysis in the range $m_{\beta\beta} < (0.071 - 0.161)$ eV [66]. There are kinematic measurements of β -decay also and the absolute effective neutrino mass is directly probed from the cut-off of the electron energy spectrum emitted from β -decay. Recent result from KATRIN experiment [67] constrains the effective electron neutrino mass m_β to be less than 1.1 eV and the latest Planck data [21] provides the upper limit on the sum of active neutrino masses $\sum m_i < 0.12$ eV. The parameters $m_{\beta\beta}$ and m_β are expressed as the sum of mass eigenstates and elements of lepton mixing matrix as [68].

$$m_{\beta\beta} = \left| \sum_{j=1}^4 |U_{ej}|^2 m_j \right|, \quad (5)$$

$$m_\beta = \left(\sum_{i=1}^4 |U_{ei}|^2 m_i^2 \right)^{1/2}. \quad (6)$$

From these, we are motivated to study a neutrino mass model based on minimal extended seesaw mechanism(MES) to explain some of the SM problems mentioned above. Several other literatures are available based on similar studies [33, 34, 60, 69–74] but the main shortcomings of such models are the presence of many hypothetical flavon fields as well as additional discrete symmetries. Particularly, in Ref.[34], the authors considered different sets of five flavons extended with another two flavons as perturbations in the Lagrangian separately for normal hierarchy(NH) and inverted hierarchy(IH). In Ref.[33], authors use S_4 symmetry as an extension to SM along with $Z_4 \times Z_3$ in Inverse Seesaw(ISS) scenario. They

consider six flavons : four S_4 triplets and two singlets, in order to generate the mass matrices in the model. The present work is different and more efficient in the fact that we use only four flavon fields ϕ, ψ, ζ and χ to construct the Dirac, Majorana and sterile neutrino mass matrices. Deviation from $\mu - \tau$ symmetry is generated through another A_4 triplet flavon η . The fields are given group charges different from other works and hence a new structure of light neutrino mass matrix is obtained using the minimal extended seesaw formula. We also consider the mass of sterile neutrino in a broader range of $(4 - 50)\text{keV}$.

The detailed description of the model is given in the next section. The structure of this paper is as follows. We present a detailed description of the model along with the mechanism for generating neutrino masses in section II followed by the numerical analysis of the model in section III. Results of the analysis is presented in section IV. We conclude with a brief summary and discussion in section V.

II. DESCRIPTION OF THE MODEL

In this model we have considered an extension of SM through $A_4 \times Z_4 \times Z_2$ where an A_4 singlet sterile neutrino S is added along with three right handed neutrino singlets $\nu_{R1}, \nu_{R2}, \nu_{R3}$. A_4 has four irreducible representations denoted by singlets $1, 1'', 1'$ and a triplet 3 . The SM lepton doublet l transforms as triplet under A_4 while the charged lepton singlets e_R, μ_R, τ_R transform as $1, 1'', 1'$ respectively. Two flavons ϕ and ψ are used along with three Higgs H, H', H'' to give neutrino masses through electroweak symmetry breaking. Another flavon η is responsible for breaking the $\mu - \tau$ symmetry of neutrino mass matrix and to generate non-zero θ_{13} . Two A_4 singlets χ and ζ are used to generate a diagonal Majorana mass matrix M_R and sterile neutrino mass matrix M_S respectively. The particle contents and their corresponding group charges are shown in Table II. Additional discrete symmetry Z_2 is used in order to remove some unwanted interactions in the Lagrangian which are otherwise allowed by $A_4 \times Z_4$, such as $\frac{1}{\Lambda}(y_m \bar{l} \tilde{H}' \psi)_1 \nu_{R1}$, $\frac{1}{\Lambda}(y_n \bar{l} \tilde{H}'' \psi)_1 S$, etc. The charged lepton and Dirac neutrino mass matrices are constructed using the Weinberg dim-5 operator[75].

The invariant Yukawa interaction terms of the model in the charged lepton sector are given by

$$-\mathcal{L}_y^{cl} \sim \frac{y_e}{\Lambda}(\bar{l}H\psi)_1 e_R + \frac{y_\mu}{\Lambda}(\bar{l}H\psi)_{1'} \mu_R + \frac{y_\tau}{\Lambda}(\bar{l}H\psi)_{1''} \tau_R \quad (7)$$

$\frac{Fields}{Charges}$	l	e_R, μ_R, τ_R	H	H'	H''	ψ	ϕ	χ	ζ	ν_{R1}	ν_{R2}	ν_{R3}	S	η
$SU(2)_L$	2	1	2	2	2	1	1	1	1	1	1	1	1	1
$U(1)_Y$	-1/2	+1	-1/2	-1/2	-1/2	1	1	0	-1	0	0	0	1	1
A_4	3	1, 1'', 1'	1	1'	1''	3	3	1	1''	1	1	1	1'	3
Z_4	1	1	1	-i	i	1	-i	1	-1	i	-1	1	-i	-i
Z_2	1	1	1	-1	1	1	1	1	-1	1	-1	1	-1	1

TABLE II. Particle content of the model and their group charges.

Whereas, the Yukawa interaction for the neutrino sector which are invariant under all the symmetry groups of the model are given by

$$\begin{aligned}
-\mathcal{L}_y^{mass} \sim & \frac{1}{\Lambda}(y_1 \bar{l} \tilde{H} \phi + y_3 \bar{l} \tilde{H} \eta)_1 \nu_{R1} + \frac{1}{\Lambda}(y_1 \bar{l} \tilde{H}' \phi + y_3 \bar{l} \tilde{H}' \eta)_1 \nu_{R2} \\
& + \frac{1}{\Lambda}(y_4 \bar{l} \tilde{H} \psi + y_2 \bar{l} \tilde{H}'' \phi + y_3 \bar{l} \tilde{H}'' \eta)_1 \nu_{R3} \\
& + \frac{1}{2} \lambda_1 \chi \bar{\nu}_{R1}^c \nu_{R1} + \frac{1}{2} \lambda_2 \chi \bar{\nu}_{R2}^c \nu_{R2} + \frac{1}{2} \lambda_3 \chi \bar{\nu}_{R3}^c \nu_{R3} \\
& + \frac{1}{2} \lambda_s \zeta \bar{S}^c \nu_{R1}
\end{aligned} \tag{8}$$

where $\tilde{H} = i\sigma_2 H^*$ is used to make the Lagrangian Gauge invariant.

After electroweak symmetry breaking, the scalar flavon fields obtain their vacuum expectation values (v.e.v.) along with alignments given as [62, 76, 77]

$$\langle \psi \rangle = v(1, 0, 0); \quad \langle \eta \rangle = v(0, 1, 0); \quad \langle \phi \rangle = v(1, 1, 1); \quad \langle \chi \rangle = v; \quad \langle \zeta \rangle = u \tag{9}$$

Using the multiplication rule of A_4 [78], the charged lepton mass matrix becomes diagonal,

$$M_L = \frac{\langle H \rangle v}{\Lambda} \text{diag}(y_e, y_\mu, y_\tau). \tag{10}$$

As a result, the charged-lepton diagonalization matrix becomes unity, $U_L = 1$. Thus, the lepton mixing matrix depends on the neutrino sector only.

From Eq.(8) using Eq.(9), the Dirac, Majorana and sterile neutrino mass matrices will take the form

$$M_D = \begin{pmatrix} a & a & c+h \\ a & a & h \\ a+t & a+t & h+t \end{pmatrix}, \quad M_R = \begin{pmatrix} d & 0 & 0 \\ 0 & e & 0 \\ 0 & 0 & f \end{pmatrix}, \tag{11}$$

$$M_s = \begin{pmatrix} g & 0 & 0 \end{pmatrix}. \quad (12)$$

where,

$$a = \frac{\langle H \rangle v}{\Lambda} y_1, \quad h = \frac{\langle H \rangle v}{\Lambda} y_2, \quad c = \frac{\langle H \rangle v}{\Lambda} y_4, \quad t = \frac{\langle H \rangle v}{\Lambda} y_3, \quad d = \lambda_1 v, \\ e = \lambda_2 v, \quad f = \lambda_3 v, \quad g = \lambda_s u.$$

In order to achieve the sterile neutrino mass in the keV range, the v.e.v of scalar χ is assumed to lie around TeV scale. An approximate estimate of the mass scales of the parameters in the model are as follows,

$$\Lambda \sim 10^{15} \text{ GeV}, \quad v \sim 10^{14} \text{ GeV}, \quad u \sim 10 \text{ TeV and } \langle H \rangle \sim 125 \text{ GeV}$$

In our analysis, we have used minimal extended seesaw(MES) mechanism to calculate the masses of active neutrino as well as sterile neutrino. In MES, the 4×4 active-sterile neutrino mass matrix is given by [79]

$$M_\nu^{4 \times 4} = - \begin{pmatrix} M_D M_R^{-1} M_D^T & M_D M_R^{-1} M_S^T \\ M_S (M_R^{-1})^T M_D^T & M_S M_R^{-1} M_S^T \end{pmatrix}. \quad (13)$$

It is important to observe that $\det(M_\nu) = 0$. Thus, at least one of the neutrino mass eigenvalues is zero in MES mechanism. Applying the seesaw condition, M_ν is further diagonalised and the (3×3) active neutrino mass matrix m_ν and the sterile neutrino mass m_s are expressed as

$$m_\nu \simeq M_D M_R^{-1} M_S^T (M_S M_R^{-1} M_S^T)^{-1} M_S (M_R^{-1})^T M_D^T - M_D M_R^{-1} M_D^T; \quad (14)$$

$$m_s \simeq - M_S M_R^{-1} M_S^T. \quad (15)$$

Using Eq.(14) and Eq.(15), the active neutrino mass matrix and the sterile neutrino mass are given by

$$m_\nu = - \begin{pmatrix} \frac{a^2}{e} + \frac{(c+h)^2}{f} & \frac{a^2}{e} + \frac{h(c+h)}{f} & \frac{a(a+t)}{e} + \frac{(c+h)(h+t)}{f} \\ \frac{a^2}{e} + \frac{h(c+h)}{f} & \frac{a^2}{e} + \frac{h^2}{f} & \frac{a(a+t)}{e} + \frac{h(h+t)}{f} \\ \frac{a(a+t)}{e} + \frac{(c+h)(h+t)}{f} & \frac{a(a+t)}{e} + \frac{h(h+t)}{f} & \frac{(a+t)^2}{e} + \frac{(h+t)^2}{f} \end{pmatrix} \quad (16)$$

and

$$m_s = -\frac{g^2}{d}. \quad (17)$$

The $\mu - \tau$ symmetry in m_ν can be realised if we put $t = 0$ in eq.(16), i.e.

$$m_\nu = - \begin{pmatrix} \frac{a^2}{e} + \frac{(c+h)^2}{f} & \frac{a^2}{e} + \frac{h(c+h)}{f} & \frac{a^2}{e} + \frac{h(c+h)}{f} \\ \frac{a^2}{e} + \frac{h(c+h)}{f} & \frac{a^2}{e} + \frac{h^2}{f} & \frac{a^2}{e} + \frac{h^2}{f} \\ \frac{a^2}{e} + \frac{h(c+h)}{f} & \frac{a^2}{e} + \frac{h^2}{f} & \frac{a^2}{e} + \frac{h^2}{f} \end{pmatrix} \quad (18)$$

III. NUMERICAL ANALYSIS

For numerical analysis, we use the latest 3σ bounds of neutrino oscillation data shown in Table 3 for both normal hierarchy(NH) and inverted hierarchy(IH). Diagonal elements of the heavy Majorana mass matrix M_R are given non-degenerate values $d = 10^{13}\text{GeV}$, $e = 10^{11}\text{GeV}$ and $f = 5 \times 10^{11}\text{GeV}$. We numerically diagonalise the active neutrino mass matrix m_ν using the relation $U^\dagger \mathcal{M} U = \text{diag}(m_1^2, m_2^2, m_3^2)$, where $\mathcal{M} = m_\nu m_\nu^\dagger$ and U is a unitary mixing matrix. For NH: $m_1 = 0$, $m_2 = \sqrt{\Delta m_{21}^2}$, and $m_3 = \sqrt{\Delta m_{21}^2 + \Delta m_{31}^2}$ and for IH: $m_1 = \sqrt{\Delta m_{21}^2 + \Delta m_{31}^2}$, $m_2 = \sqrt{\Delta m_{21}^2}$, and $m_3 = 0$, where $\Delta m_{ij}^2 = |m_j^2 - m_i^2|$. We can also define a parameter r which is given by the ratio between the mass squared differences as

$$r = \sqrt{\frac{\Delta m_{21}^2}{\Delta m_{31}^2}} = \frac{m_2}{m_3} \quad \text{for NH} \quad (19)$$

and

$$r = \sqrt{\frac{\Delta m_{21}^2}{|\Delta m_{32}^2|}} = \sqrt{1 - \frac{m_1^2}{m_2^2}} \quad \text{for IH} \quad (20)$$

In PDG convention [4], U is parameterised using three mixing angles $\theta_{12}, \theta_{13}, \theta_{23}$, one Dirac phase δ_{CP} and two Majorana phases α, β . The values of α and β are unknown and they are randomly varied in the range $(0, 2\pi)$. The light neutrino mass matrix m_ν contains four unknown complex parameters a, c, t and h . We randomly choose the values of these parameters in the ranges given in Table III. The parameter space is constrained by upper bound on the sum of active neutrino mass $\sum m_i < 0.12 \text{ eV}$ and the 3σ bounds of the neutrino mixing angles. The ratio r is independent of the mass scales and mixing matrix U . From Table I, the best-fit value of r in NH is $r_o = 0.172$. The allowed parameter space is further constrained by the experimental values of r .

The full (4×4) active-sterile mass matrix is diagonalised by a unitary (4×4) mixing matrix given by [80]

$$V \simeq \begin{pmatrix} (1 - \frac{1}{2}RR^\dagger)U & R \\ -R^\dagger U & 1 - \frac{1}{2}R^\dagger R \end{pmatrix}, \quad (21)$$

where R represents the strength of active-sterile mixing given by

$$R = M_D M_R^{-1} M_S^T (M_S M_R^{-1} M_S^T)^{-1} = \begin{pmatrix} \frac{a}{g} \\ \frac{a}{g} \\ \frac{a+t}{g} \end{pmatrix} \quad (22)$$

We can solve the neutrino mixing angles from the elements of active-sterile mixing matrix V [81, 82]. However, The deviation from unitarity of the 3×3 mixing matrix U is given by $\frac{1}{2}|RR^\dagger|$ and it is found to be very small $\leq \mathcal{O}(10^{-10})$. As a result, we can ignore the effects of the keV-scale sterile neutrino in the mixing matrix U . Neutrino mixing angles are obtained from U using the general formula given below

$$\sin^2 \theta_{13} = |U_{13}|^2, \quad \sin^2 \theta_{12} = \frac{|U_{12}|^2}{1 - |U_{13}|^2}, \quad \sin^2 \theta_{23} = \frac{|U_{23}|^2}{1 - |U_{13}|^2} \quad (23)$$

In order to study the possibility of keV-scale sterile neutrino as a dark matter, it is required that the active-sterile mixing angle is very small, $\theta_s < 10^{-6}$. Remaining parameter g is solved by constraining the sterile neutrino mass in the range $(4 - 50)$ keV.

Besides, one of the most important parameters in neutrino sector is the Jarlskog invariant J . Dirac CP violating phase δ_{CP} is related to J and it is given by

$$J = \text{Im}[U_{e1}U_{\mu 2}U_{e2}^*U_{\mu 1}^*] = s_{23}c_{23}s_{12}c_{12}s_{13}c_{13}^2 \sin \delta_{CP} \quad (24)$$

where $s_{ij} = \sin \theta_{ij}$ and $c_{ij} = \cos \theta_{ij}$ are the neutrino mixing angles calculated from the model. Similarly, the Majorana phases are also evaluated from U using the invariants I_1 and I_2 defined as follows

$$I_1 = \text{Im}[U_{e1}^*U_{e2}] = c_{12}s_{12}c_{13}^2 \sin(\alpha/2), \quad (25)$$

$$I_2 = \text{Im}[U_{e1}^*U_{e3}] = c_{12}s_{12}c_{13} \sin\left(\frac{\beta}{2} - \delta_{CP}\right) \quad (26)$$

To find the best-fit values of the free parameters in our model as well as the neutrino observables, we use the χ^2 function given by

$$\chi^2(x_i) = \sum_j \left(\frac{y_j(x_i) - y_j^{bf}}{\sigma_j} \right)^2 \quad (27)$$

where x_i are the free parameters in the model and j is summed over the observables $\{\sin^2 \theta_{12}, \sin^2 \theta_{13}, \sin^2 \theta_{23}, r\}$. $y_j(x_i)$ denotes the model predictions for the observables and

Parameters	Allowed ranges (GeV)	Best-fit (GeV)	Parameter phases	Best-fit
$ a $	0.46 - 0.60	0.574	$\phi_a = (0, 2\pi)$	0.59 π
$ c $	2.53 - 4.72	3.835	$\phi_c = (0, 2\pi)$	0.44 π
$ t $	0.80 - 1.59	0.949	$\phi_t = (0, 2\pi)$	2.19 π
$ h $	3.20 - 3.94	3.469	$\phi_h = (0, 2\pi)$	-2.98 π

TABLE III. Allowed ranges of model parameters and their best-fit values corresponding to χ_{min}^2 .

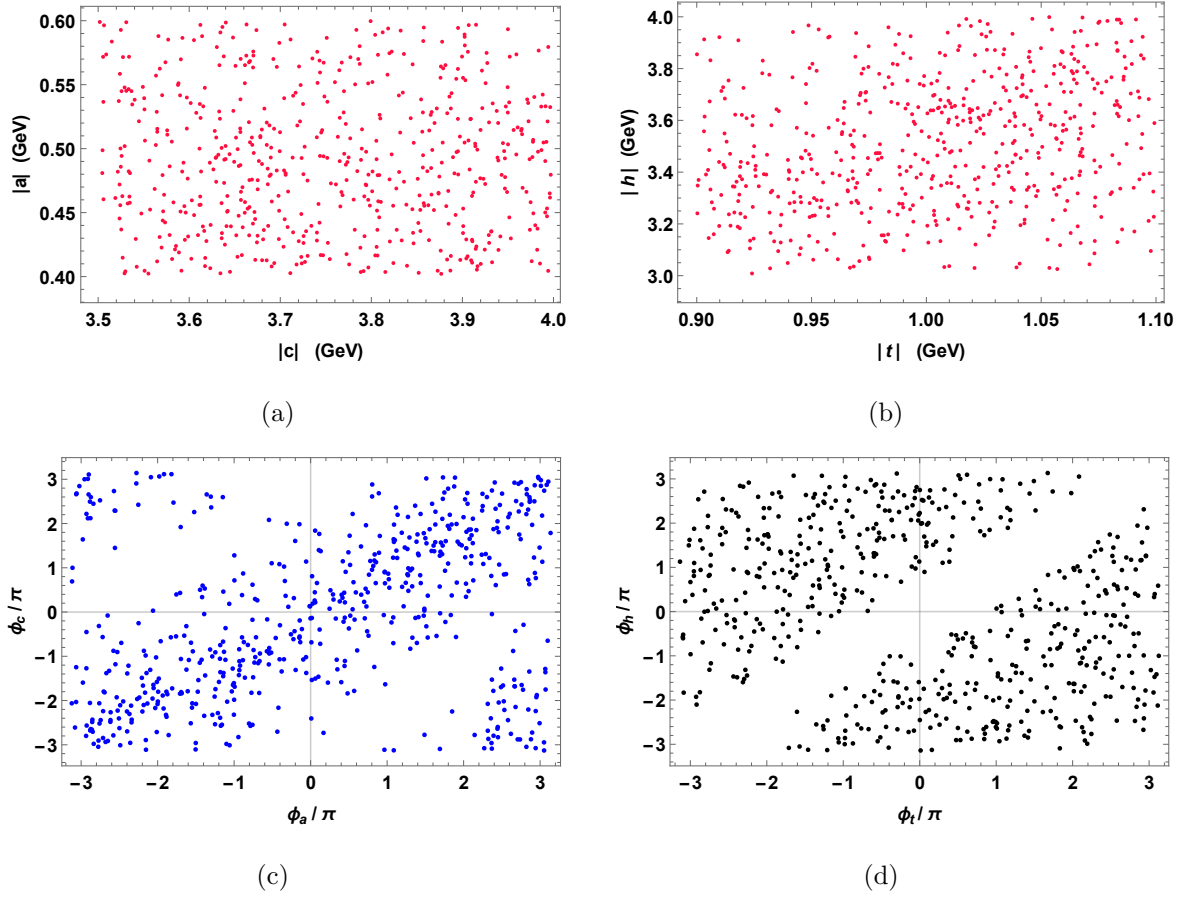


FIG. 1. (a),(b). Variation among allowed model parameters. (c),(d). Variation between the allowed phases of the parameters.

y_j^{bf} are their best-fit values obtained from the global analysis. σ_j denotes the corresponding uncertainties obtained by symmetrizing 1σ range of the neutrino observables given in table I. By minimizing the overall χ^2 function, we can calculate the best-fit values of our model parameters.

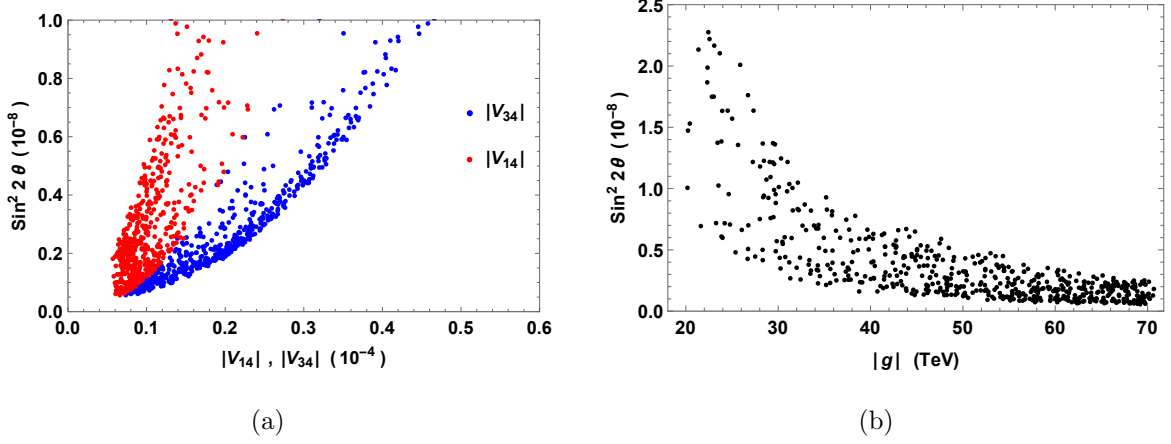


FIG. 2. (a). Variations of effective mixing angle $\sin^2 2\theta$ with elements of active-sterile mixing strength R . (b) Variation of $\sin^2 2\theta$ with $|g|$.

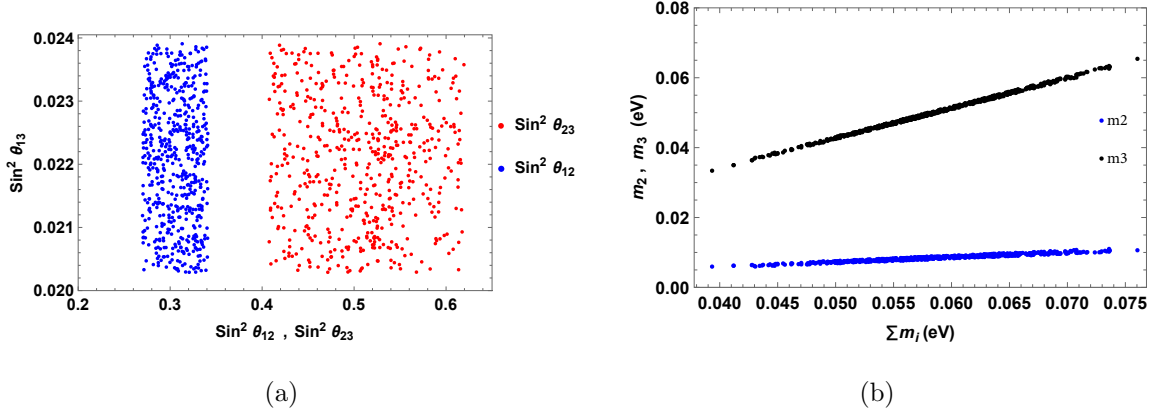


FIG. 3. (a). Plot between mixing angle $\sin^2 \theta_{13}$ with $\sin^2 \theta_{12}$ and $\sin^2 \theta_{23}$. (b) Variation of m_1 and m_2 with $\sum m_i$.

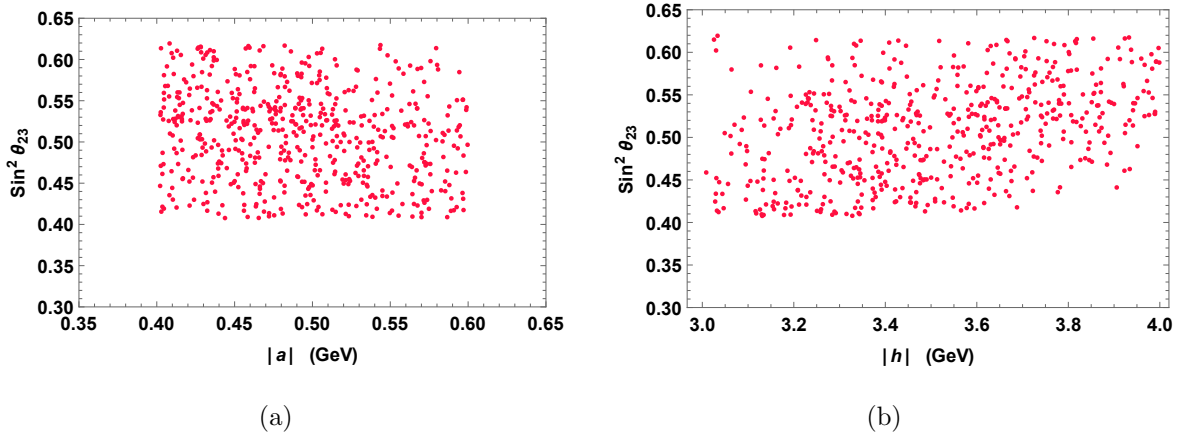


FIG. 4. Plot between mixing angle $\sin^2 \theta_{13}$ with model parameters $|a|$ and $|h|$.

IV. RESULTS

For the given ranges of the parameters in Table III, our model is compatible with global fit results of the neutrino oscillation parameters at 3σ level for NH only, while IH is disallowed at 3σ level. The variation between model parameters allowed in the numerical analysis for NH are shown in Fig.1 (a),(b). The phases of the allowed parameters are shown as scatter plots in Fig.1 (c),(d). It is observed that the allowed parameter space is very narrow for a and t compared to c and h . Fig.3 (b) shows the plot between active neutrino masses m_2 and m_3 with the sum of neutrino masses $\sum m_i$. For NH, $m_1 = 0$ and upper bound on the sum of neutrino mass is obtained at $\sum m_i \leq 0.07604$ eV while the maximum values of m_2 and m_3 are found to be respectively 0.01103 eV and 0.06541 eV. From the χ^2 analysis, we find that the best fit values of the model parameters for $\chi^2_{min} = 0.8575$ in NH are obtained at $|a| = 5.74 \times 10^8 \text{eV}$, $|c| = 3.83 \times 10^9 \text{eV}$, $|t| = 9.49 \times 10^8 \text{eV}$ and $|h| = 3.47 \times 10^9 \text{eV}$ while the respective best-fit values of their phases are obtained at $\phi_a = 0.591\pi$, $\phi_c = 0.443\pi$, $\phi_t = 2.19\pi$ and $\phi_h = -2.98\pi$. Corresponding best-fit values of neutrino observables are found to be $\sin^2 \theta_{12} = 0.30110$, $\sin^2 \theta_{13} = 0.02212$, $\sin^2 \theta_{23} = 0.55542$ and $r = 0.17466$. The complete parameter ranges and their best-fit values determined from the numerical analysis of the model are shown in Table III. Effective active-sterile mixing angle $\sin^2 2\theta$ as a function of parameter $|g|$ and mixing matrix element $|V_{14}|, |V_{34}|$ are shown in Fig.2.

For the charged lepton sector, by comparing Eq.(10) with the experimental values for masses of the charged leptons given in Ref.[4], $m_e = 0.51099$ MeV, $m_\mu = 105.65837$ MeV, $m_\tau = 1776.86$ MeV, we get the charged lepton Yukawa constants as $y_e \sim 10^{-5}$, $y_\mu \sim 10^{-3}$ and $y_\tau \sim 10^{-2}$.

A. Mixing angles and phases δ_{CP} , α and β

The variation plot among neutrino mixing angles $\sin^2 \theta_{12}$, $\sin^2 \theta_{23}$ with $\sin^2 \theta_{13}$ is shown in Fig.3(a). Values of $\sin^2 \theta_{23}$ are distributed within the 3σ range with very small crowding towards region above 0.5. Future generation neutrino oscillation experiments such as JUNO [83], Hyper-Kamiokande [84], DUNE [85], etc. will hopefully confirm the neutrino mass ordering and also determine the octant degeneracy of θ_{23} . However, data points for $\sin^2 \theta_{13}$ and $\sin^2 \theta_{12}$ are equally distributed within their 3σ ranges. In order to show the variation of

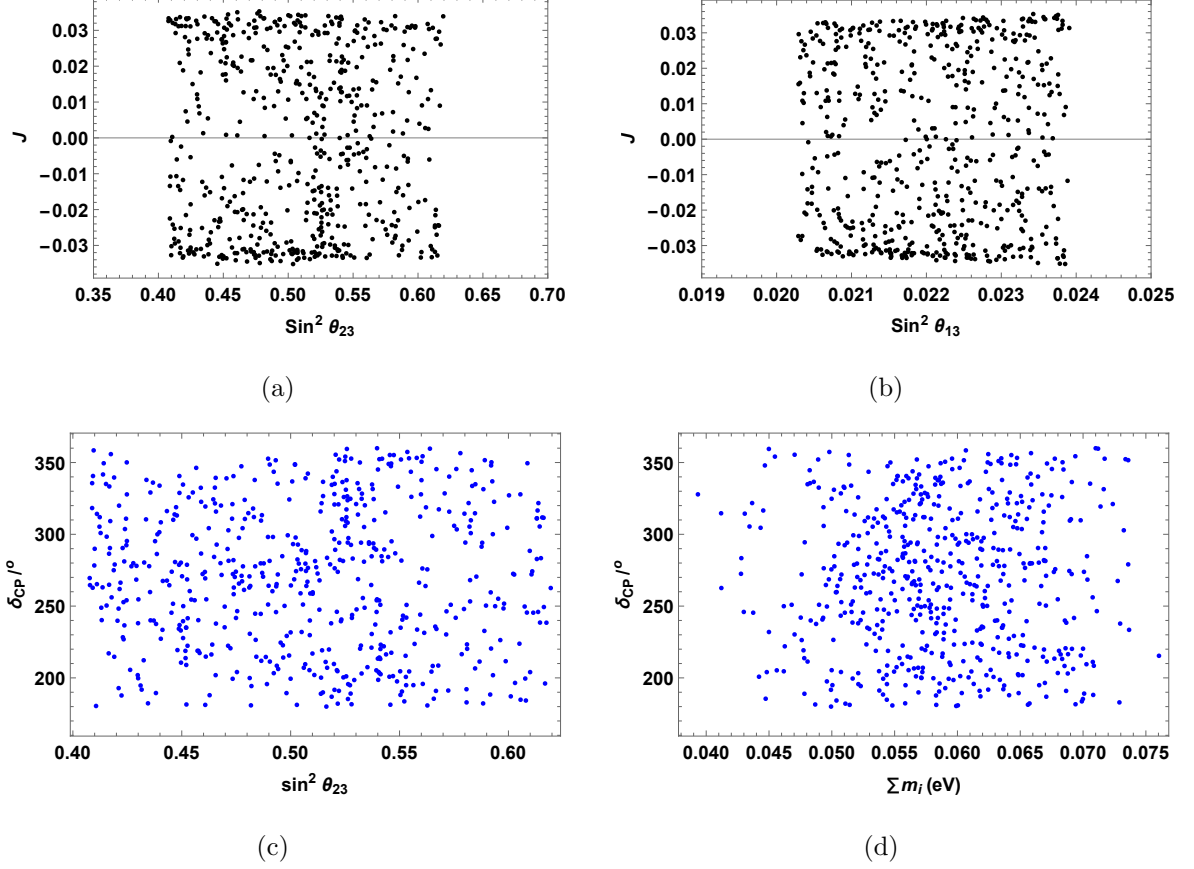


FIG. 5. (a),(b). Plot between mixing angles $\sin^2 \theta_{13}$ and $\sin^2 \theta_{23}$ with J . (c),(d). Variation of CP-violating Dirac phase δ_{CP} with $\sin^2 \theta_{23}$ and $\sum m_i$.

neutrino mixing angles as a function of the model parameters, we have plotted $\sin^2 \theta_{23}$ with the model parameters $|a|$ and $|h|$ in Fig.4. It can be observed that larger value of $|h|$ results in larger values of $\sin^2 \theta_{23}$ whereas values of $\sin^2 \theta_{23}$ does not show any distinct correlation with parameter a .

Dirac CP-violating phase δ_{CP} is calculated through the Jarlskog invariant J as given in Eq. (24). We have plotted J as a function of $\sin^2 \theta_{23}$ and $\sin^2 \theta_{13}$ in Fig.5 (a),(b). Values of J determined from the model lie within the range ± 0.0352 . Fig.5 (c),(d) show the plot between δ_{CP} with $\sin^2 \theta_{23}$ and $\sum m_i$ respectively. We obtain the Dirac CP-violating phase in the range $180.01^\circ \leq \delta_{CP} \leq 359.96^\circ$. The best fit-value of δ_{CP} is obtained at 326.09° . Fig.6 shows the predictions of Majorana phases α and β .

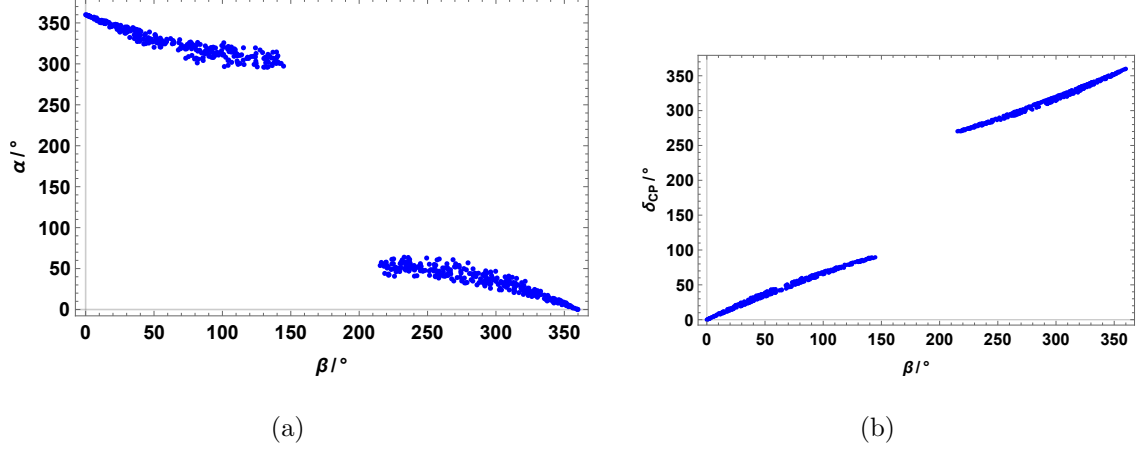


FIG. 6. (a). Plot between the Majorana phases α and β . (b) Variation of δ_{CP} with Majorana phase β .

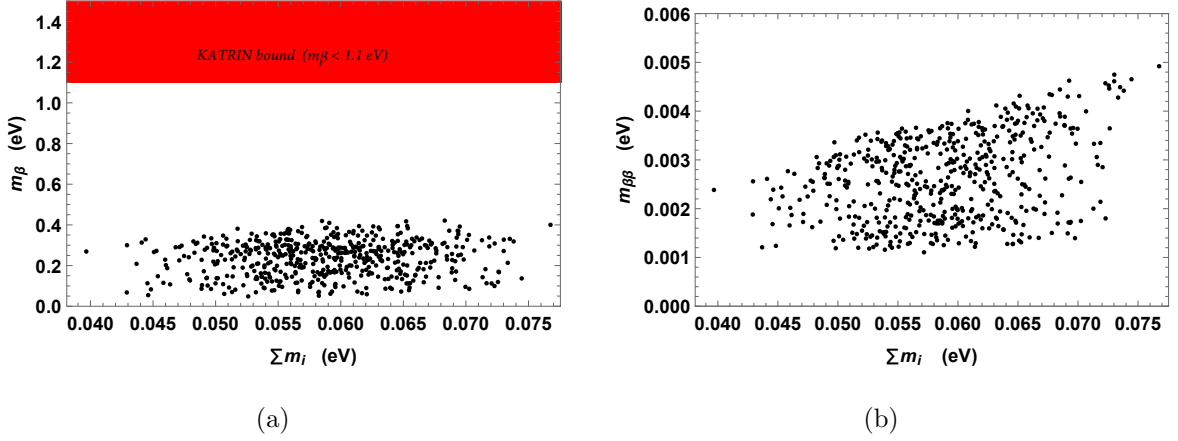


FIG. 7. (a). Plot between effective electron mass m_β with $\sum m_i$. The coloured strip shows the upper bound from latest KATRIN data $m_\beta < 1.1$ eV. (b) Variation of effective neutrino mass $m_{\beta\beta}$ with $\sum m_i$.

B. Effective masses m_β and $m_{\beta\beta}$ from β -decay and $0\nu\beta\beta$

The effective neutrino mass and effective electron mass are calculated from $0\nu\beta\beta$ and β -decay experiments using Eq.(5) and Eq.(6) respectively. Variations of $m_{\beta\beta}$ and m_β with sum of active neutrino masses $\sum m_i$ are shown in Fig.7. From these plots, we observe that the effective mass parameter lies in the range $m_{\beta\beta} \sim (0.9794 - 5.0291)$ meV which will be a great challenge for future $0\nu\beta\beta$ experiments [86, 87]. On the other hand, Fig7.(a) indicates that the effective electron mass is obtained in the range $m_\beta \sim (0.0845 - 0.4103)$ eV which well below the upper bound provided by the latest KATRIN experiment [67].

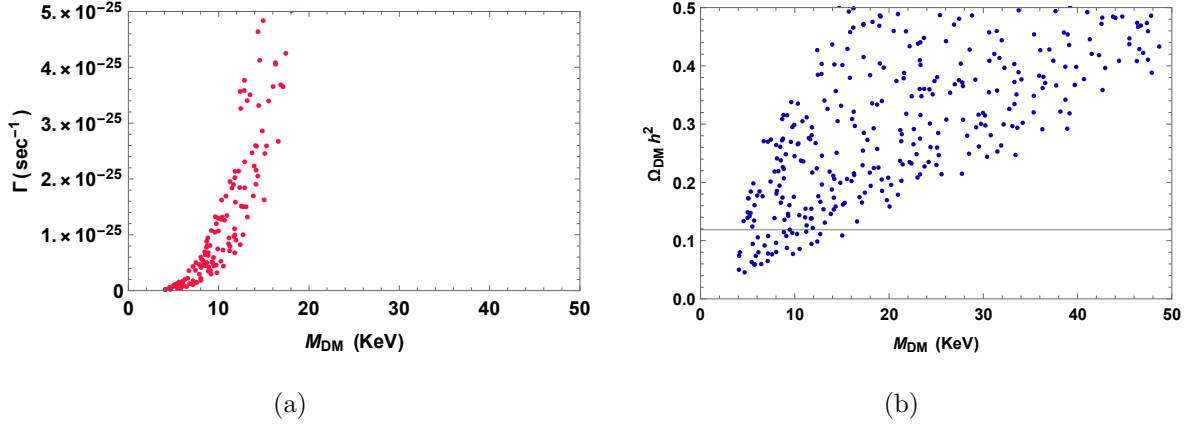


FIG. 8. (a) Variation of decay width Γ with mass of the sterile neutrino $m_s \equiv M_{DM}$. (b) Variation of relic density $\Omega_{DM}h^2$ with mass of sterile neutrino. Here, the horizontal line represents the experimental data of relic abundance of DM in the Universe which is 0.1187 ± 0.0017

C. Dark matter

Assuming the existence of keV-scale sterile neutrinos, we work out the possibilities of it behaving as a dark matter candidate. We have used the relation for relic density and decay width from Eq.(3) and Eq.(2) respectively to check the validity of the present model in giving the observed DM density. Fig.8 (a) shows the plot between decay width Γ with the mass of sterile neutrino $m_s \equiv M_{DM}$. In our analysis, we have considered the upper limit of decay width to be $\mathcal{O}(10^{-25})\text{sec}^{-1}$ for the sterile neutrino to behave as a dark matter. From Fig.8 (a), it is found that the allowed mass range for sterile neutrino is $m_s \leq 20$ keV. This range of m_s corresponds to the effective mixing angle $\sim \mathcal{O}(10^{-11} - 10^{-9})$. Comparing with the results of the analysis in Ref.[88] shown in Fig.9(a), we can observe that the narrow mass range $m_s \leq 20$ keV corresponding to effective mixing angle $\mathcal{O} \sim (10^{-10} - 10^{-11})$ is still allowed by the various experimental bounds. This observation may also supplement the unknown observation of 3.5 keV signal in X-ray data from the decay of a 7 keV sterile neutrino[25, 53]. Similarly, based on the plots of decay width $\Omega_{DM}h^2$ in Fig.8(b), we find that the allowed mass of sterile neutrino in a more constrained range of (4 – 18) keV is observed to be giving the correct abundance consistent with current experimental value given in Eq.(1).

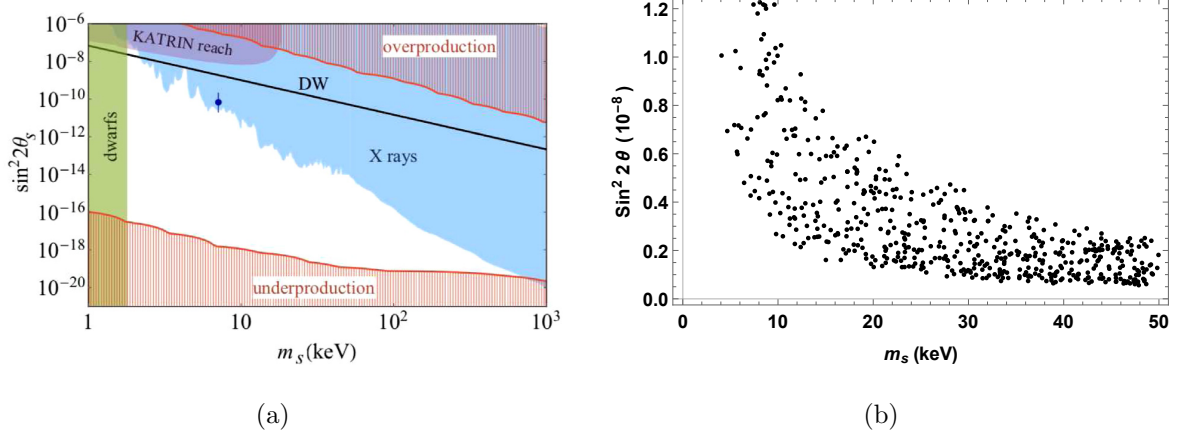


FIG. 9. (a). Various bounds on the mass and effective mixing angle of the keV sterile neutrino DM. This plot is taken as reference from Ref.[88]. (b) Variation of effective mixing angle $\sin^2 2\theta$ with mass of sterile neutrino m_s .

D. Baryogenesis via Leptogenesis

We have considered non-degenerate masses of heavy right-handed neutrinos such that $e < f \ll d$, i.e. ν_{R2} is the lightest in our case. The lightest ν_{R2} can decay into a Higgs and lepton pair which will produce sufficient lepton asymmetry giving rise to the experimentally observed baryon asymmetry of the Universe. We have used the parameterization from Ref. [89] and the baryon asymmetry is given by

$$Y_B = ck \frac{\epsilon_{22}}{g_*} \quad (28)$$

where $c \sim 12/37$ is a constant that determines the fraction of lepton asymmetry converted to baryon asymmetry. k is the dilution factor which can be parameterized in our model as

$$k \simeq \frac{0.3}{K(\ln K)^{0.6}} \quad (29)$$

where K is defined as

$$K = \frac{\Gamma}{H(T = M_2)} = \frac{(\lambda^\dagger \lambda)_{22} M_2}{8\pi} \frac{M_{Planck}}{1.66 \sqrt{g_*} M_2^2} \quad (30)$$

Here, Γ is the decay width of ν_{R2} . Further, g_* is the massless relativistic degree of freedom in the thermal bath and it is approximately 110. Finally, ϵ_{22} is the lepton asymmetry produced in the decay of the lightest ν_{R2} . It is given by

$$\epsilon_{22} = \frac{\Gamma(\nu_{R2} \rightarrow l_L + \bar{\phi}) - \Gamma(\nu_{R2} \rightarrow \bar{l}_L + \phi)}{\Gamma(\nu_{R2} \rightarrow l_L + \bar{\phi}) + \Gamma(\nu_{R2} \rightarrow \bar{l}_L + \phi)} \quad (31)$$

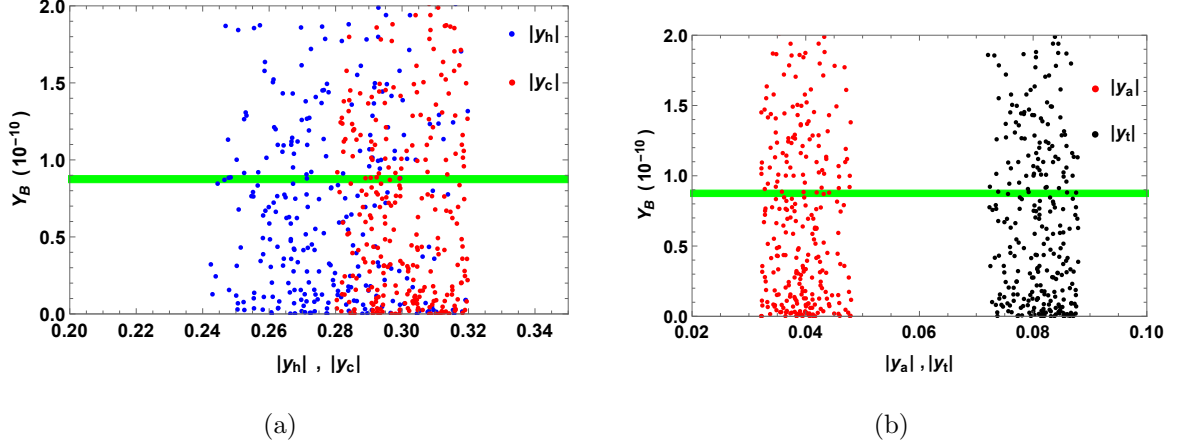


FIG. 10. Plot between Baryon asymmetry parameter Y_B with the Yukawa couplings present in the lepton sector of the model. The green strip represents the experimental bound of Y_B which is $(8.7 \pm 0.06) \times 10^{-11}$.

The lepton asymmetry is calculated as [89–92]

$$\epsilon_{22} = \frac{1}{8\pi} \frac{1}{(\lambda^\dagger \lambda)_{22}} \sum_j^{1,3} \text{Im}[(\lambda^\dagger \lambda)_{2j}]^2 g(x_j) \quad (32)$$

where $x_j \equiv \frac{M_j^2}{M_2^2}$ and within the SM [90] $g(x_j)$ is defined as,

$$g(x_j) = \sqrt{x_j} \left(\frac{2 - x_j - (1 - x_j^2) \ln((1 + x_j)/x_j)}{1 - x_j} \right) \quad (33)$$

In the above relations, λ is the Yukawa matrix corresponding to the Dirac mass matrix Eq.(11). We constructed the Yukawa matrix λ from the model parameters a, c, h and t . We have solved Y_B using these relations and the variation plots of Y_B with Yukawa constants are shown in Fig.10. In our analysis, the Yukawa constants of the lepton sector are observed to be $\mathcal{O}(10^{-2} - 10^{-1})$ which are in the acceptable range of the perturbativity limit $y \leq \sqrt{4\pi}$. The model parameters and their respective Yukawa couplings are found to give observed experimental bound for Baryon asymmetry Y_B .

V. SUMMARY AND DISCUSSION

We have successfully developed a neutrino mass model based on the extension of SM using $A_4 \times Z_4 \times Z_2$ symmetry. We use the Weinberg dimension five operator to construct the neutrino mass matrices in the model. Possibility of a keV scale sterile neutrino to behave as a dark matter is studied using MES mechanism. The mass of the sterile neutrino is constrained

in the range $(4-50)\text{keV}$. We solved the model parameters using the 3σ values of the neutrino observables. It is observed that the model parameters can produce an effective active-sterile mixing $\sin^2 \theta \leq 10^{-6}$ which is a requirement for sterile neutrino to be DM. We are able to reproduce neutrino oscillation parameters within their 3σ range including the Planck bound on the sum of active neutrinos $\sum m_i < 0.12\text{eV}$. Other phenomenological studies such as effective neutrino mass and effective electron mass from $0\nu\beta\beta$ and β -decay experiments, Baryogenesis via Leptogenesis, etc. are carried out to check the validity of our model. The effective mass parameter $m_{\beta\beta}$ is observed to be in the range $\sim (0.9794 - 5.0291)\text{meV}$ while effective neutrino mass is found to be $m_\beta \sim (0.0845 - 0.4103)\text{eV}$ which is less than the upper bound of latest KATRIN data. The keV sterile neutrino mass in range $m_s \sim (4 - 18)\text{keV}$ is found to give the correct abundance as well as decay width for a DM particle. Baryogenesis via leptogenesis is studied from the lepton asymmetry produced by the decay of the lightest Majorana right-handed neutrino which is ν_{R2} in our case. The experimental value of Baryon asymmetry Y_B is found to be consistent for a very small range of Yukawa couplings y_a, y_c, y_t and y_t . We have also determined the best-fit values of the model parameters as well as the neutrino observables using the χ^2 analysis. Further, it is important to note that our analysis is found to be consistent with the global analysis of neutrino oscillation data for NH only while IH is excluded at the 3σ level. In fact, for the given parameter space that we considered, the neutrino observables such as r , gives larger values outside the 3σ . Hence, IH case is disallowed in this model structure with the given parameter space. However, it may be checked by considering a different set of parameter spaces or by making a small change in the structure of the model through new flavons [62, 74, 79], which can be studied in future. In conclusion, we have presented a model which provides a well-motivated DM candidate as well as consistent neutrino phenomenologies.

ACKNOWLEDGMENTS

One of the authors (MKS), would like to thank DST-INSPIRE, Govt. of India, for providing financial support under DST-INSPIRE Fellowship (IF180349).

- [1] Q. R. Ahmad, Allen, et al. Measurement of day and night neutrino energy spectra at sno and constraints on neutrino mixing parameters. *Phys. Rev. Lett.*, 89:011302, Jun 2002.
- [2] SnO Collaboration et al. Direct evidence for neutrino flavor transformation from neutral-current interactions in the sudbury neutrino observatory. *arXiv preprint nucl-ex/0204008*, 2002.
- [3] Ko Abe, Y Haga, Y Hayato, M Ikeda, K Iyogi, J Kameda, Y Kishimoto, M Miura, S Moriyama, M Nakahata, et al. Limits on sterile neutrino mixing using atmospheric neutrinos in super-kamiokande. *Physical Review D*, 91(5):052019, 2015.
- [4] R. L. Workman and Others. Review of Particle Physics. *PTEP*, 2022:083C01, 2022.
- [5] A Aguilar-Arevalo, LSND collaboration, et al. Evidence for neutrino oscillations from the observation of anti-neutrino (electron) appearance in a anti-neutrino (muon) beam. *Phys. Rev. D*, 64:112007, 2001.
- [6] AA Aguilar-Arevalo, BC Brown, L Bugel, G Cheng, JM Conrad, RL Cooper, R Dharmapalan, A Diaz, Z Djurcic, DA Finley, et al. Significant excess of electronlike events in the miniboone short-baseline neutrino experiment. *Physical review letters*, 121(22):221801, 2018.
- [7] CA Argüelles, I Esteban, M Hostert, Kevin J Kelly, J Kopp, PAN Machado, I Martinez-Soler, and YF Perez-Gonzalez. Microboone and the ν e interpretation of the miniboone low-energy excess. *Physical Review Letters*, 128(24):241802, 2022.
- [8] Ivan Esteban, M.C. Gonzalez-Garcia, Michele Maltoni, Thomas Schwetz, and Albert Zhou. The fate of hints: updated global analysis of three-flavor neutrino oscillations. *Journal of High Energy Physics*, 2020(9), Sep 2020.
- [9] Douglas Clowe, Maruša Bradač, Anthony H Gonzalez, Maxim Markevitch, Scott W Randall, Christine Jones, and Dennis Zaritsky. A direct empirical proof of the existence of dark matter. *The Astrophysical Journal*, 648(2):L109, 2006.

- [10] Marco Battaglieri, Alberto Belloni, Aaron Chou, Priscilla Cushman, Bertrand Echenard, Rouven Essig, Juan Estrada, Jonathan L Feng, Brenna Flaughner, Patrick J Fox, et al. Us cosmic visions: new ideas in dark matter 2017: community report. *arXiv preprint arXiv:1707.04591*, 2017.
- [11] Marco Taoso, Gianfranco Bertone, and Antonio Masiero. Dark matter candidates: a ten-point test. *Journal of Cosmology and Astroparticle Physics*, 2008(03):022, 2008.
- [12] Alexander Merle. kev sterile neutrino dark matter and neutrino model building. *Journal of Physics: Conference Series*, 375(1):012047, jul 2012.
- [13] Alexander Merle. kev sterile neutrino dark matter. *arXiv preprint arXiv:1702.08430*, 2017.
- [14] Basudeb Dasgupta and Joachim Kopp. Sterile neutrinos. *Physics Reports*, 928:1–63, 2021.
- [15] Peter AR Ade, Aghanim, et al. Planck 2015 results-xiii. cosmological parameters. *Astronomy & Astrophysics*, 594:A13, 2016.
- [16] Scott Dodelson and Lawrence M Widrow. Sterile neutrinos as dark matter. *Physical Review Letters*, 72(1):17, 1994.
- [17] Xiangdong Shi and George M Fuller. New dark matter candidate: Nonthermal sterile neutrinos. *Physical Review Letters*, 82(14):2832, 1999.
- [18] Palash B Pal and Lincoln Wolfenstein. Radiative decays of massive neutrinos. *Physical Review D*, 25(3):766, 1982.
- [19] Kenny CY Ng, Brandon M Roach, Kerstin Perez, John F Beacom, Shunsaku Horiuchi, Roman Krivonos, and Daniel R Wik. New constraints on sterile neutrino dark matter from nustar m31 observations. *Physical Review D*, 99(8):083005, 2019.
- [20] Asmaa Abada, Giorgio Arcadi, and Michele Lucente. Dark matter in the minimal inverse seesaw mechanism. *Journal of Cosmology and Astroparticle Physics*, 2014(10):001, 2014.
- [21] Nabila Aghanim, Yashar Akrami, Mark Ashdown, J Aumont, C Baccigalupi, M Ballardini, AJ Banday, RB Barreiro, N Bartolo, S Basak, et al. Planck 2018 results-vi. cosmological parameters. *Astronomy & Astrophysics*, 641:A6, 2020.
- [22] Aurel Schneider. Astrophysical constraints on resonantly produced sterile neutrino dark matter. *Journal of Cosmology and Astroparticle Physics*, 2016(04):059, 2016.
- [23] Alexey Boyarsky, A Neronov, Oleg Ruchayskiy, and M Shaposhnikov. Constraints on sterile neutrinos as dark matter candidates from the diffuse x-ray background. *Monthly Notices of the Royal Astronomical Society*, 370(1):213–218, 2006.

- [24] Kevork N. Abazajian, Maxim Markevitch, Savvas M. Koushiappas, and Ryan C. Hickox. Limits on the radiative decay of sterile neutrino dark matter from the unresolved cosmic and soft x-ray backgrounds. *Phys. Rev. D*, 75:063511, Mar 2007.
- [25] Ezra Bulbul, Maxim Markevitch, Adam Foster, Randall K Smith, Michael Loewenstein, and Scott W Randall. Detection of an unidentified emission line in the stacked x-ray spectrum of galaxy clusters. *The Astrophysical Journal*, 789(1):13, 2014.
- [26] Norio Sekiya, Noriko Y. Yamasaki, and Kazuhisa Mitsuda. A search for a keV signature of radiatively decaying dark matter with Suzaku XIS observations of the X-ray diffuse background. *Publications of the Astronomical Society of Japan*, 68(SP1), 09 2015. S31.
- [27] Julien Baur, Nathalie Palanque-Delabrouille, Christophe Yèche, Christophe Magneville, and Matteo Viel. Lyman-alpha forests cool warm dark matter. *Journal of Cosmology and Astroparticle Physics*, 2016(08):012, 2016.
- [28] Scott Tremaine and James E Gunn. Dynamical role of light neutral leptons in cosmology. *Physical Review Letters*, 42(6):407, 1979.
- [29] Alexey Boyarsky, Oleg Ruchayskiy, and Dmytro Iakubovskyi. A lower bound on the mass of dark matter particles. *Journal of Cosmology and Astroparticle Physics*, 2009(03):005, 2009.
- [30] Carlos A Argüelles, Vedran Brdar, and Joachim Kopp. Production of keV sterile neutrinos in supernovae: New constraints and gamma-ray observables. *Physical Review D*, 99(4):043012, 2019.
- [31] Maximilian Berbig. Freeze-In of radiative keV-scale neutrino dark matter from a new $U(1)_{B-L}$. *JHEP*, 09:101, 2022.
- [32] Alexey Boyarsky, Julien Lesgourgues, Oleg Ruchayskiy, and Matteo Viel. Realistic sterile neutrino dark matter with keV mass does not contradict cosmological bounds. *Phys. Rev. Lett.*, 102:201304, May 2009.
- [33] Nayana Gautam and Mrinal Kumar Das. Phenomenology of keV scale sterile neutrino dark matter with S_4 flavor symmetry. *JHEP*, 01:098, 2020.
- [34] Pritam Das and Mrinal Kumar Das. Phenomenology of keV sterile neutrino in minimal extended seesaw. *Int. J. Mod. Phys. A*, 35(22):2050125, 2020.
- [35] Carlos Jaramillo. Reviving keV sterile neutrino dark matter. *JCAP*, 10:093, 2022.
- [36] Rathin Adhikari, M Agostini, N Anh Ky, T Araki, M Archidiacono, M Bahr, J Baur, J Behrens, F Bezrukov, PS Bhupal Dev, et al. A white paper on keV sterile neutrino dark

- matter. *Journal of cosmology and astroparticle physics*, 2017(01):025, 2017.
- [37] Kevork N Abazajian. Sterile neutrinos in cosmology. *Physics Reports*, 711:1–28, 2017.
 - [38] Alexander Kusenko. Sterile neutrinos: the dark side of the light fermions. *Physics Reports*, 481(1-2):1–28, 2009.
 - [39] André De Gouvêa, Manibrata Sen, Walter Tangarife, and Yue Zhang. Dodelson-Widrow Mechanism in the Presence of Self-Interacting Neutrinos. *Phys. Rev. Lett.*, 124(8):081802, 2020.
 - [40] A. Boyarsky, A. Neronov, O. Ruchayskiy, M. Shaposhnikov, and I. Tkachev. Strategy for searching for a dark matter sterile neutrino. *Phys. Rev. Lett.*, 97:261302, Dec 2006.
 - [41] Alexey Boyarsky, Dmytro Iakubovskiy, Oleg Ruchayskiy, and Vladimir Savchenko. Constraints on decaying dark matter from XMM–Newton observations of M31. *Monthly Notices of the Royal Astronomical Society*, 387(4):1361–1373, 07 2008.
 - [42] Oleg Ruchayskiy, Alexey Boyarsky, Dmytro Iakubovskiy, Esra Bulbul, Dominique Eckert, Jeroen Franse, Denys Malyshev, Maxim Markevitch, and Andrii Neronov. Searching for decaying dark matter in deep XMM–Newton observation of the Draco dwarf spheroidal. *Monthly Notices of the Royal Astronomical Society*, 460(2):1390–1398, 05 2016.
 - [43] Casey R Watson, Zhiyuan Li, and Nicholas K Polley. Constraining sterile neutrino warm dark matter with chandra observations of the andromeda galaxy. *Journal of Cosmology and Astroparticle Physics*, 2012(03):018, 2012.
 - [44] Signe Riemer-Sørensen. Constraints on the presence of a 3.5 keV dark matter emission line from chandra observations of the galactic centre. *Astronomy & Astrophysics*, 590:A71, 2016.
 - [45] F Hofmann, JS Sanders, K Nandra, N Clerc, and MASSIMO Gaspari. 7.1 keV sterile neutrino constraints from x-ray observations of 33 clusters of galaxies with chandra acis. *Astronomy & Astrophysics*, 592:A112, 2016.
 - [46] Alexander Kusenko, Michael Loewenstein, and Tsutomu T. Yanagida. Moduli dark matter and the search for its decay line using suzaku x-ray telescope. *Phys. Rev. D*, 87:043508, Feb 2013.
 - [47] O. Urban, N. Werner, S. W. Allen, A. Simionescu, J. S. Kaastra, and L. E. Strigari. A Suzaku search for dark matter emission lines in the X-ray brightest galaxy clusters. *Monthly Notices of the Royal Astronomical Society*, 451(3):2447–2461, 06 2015.

- [48] N. Mirabal. Swift observation of Segue 1: constraints on sterile neutrino parameters in the darkest galaxy. *Monthly Notices of the Royal Astronomical Society: Letters*, 409(1):L128–L131, 11 2010.
- [49] Andrii Neronov, Denys Malyshev, and Dominique Eckert. Decaying dark matter search with nustar deep sky observations. *Physical Review D*, 94(12):123504, 2016.
- [50] S. Riemer-Sørensen, D. Wik, G. Madejski, S. Molendi, F. Gastaldello, F. A. Harrison, W. W. Craig, C. J. Hailey, S. E. Boggs, F. E. Christensen, D. Stern, W. W. Zhang, and A. Hornstrup. Dark matter line emission constraints from nustar observations of the bullet cluster. *The Astrophysical Journal*, 810(1):48, aug 2015.
- [51] Kerstin Perez, Kenny CY Ng, John F Beacom, Cora Hersh, Shunsaku Horiuchi, and Roman Krivonos. Almost closing the ν msm sterile neutrino dark matter window with nustar. *Physical Review D*, 95(12):123002, 2017.
- [52] Esra Bulbul, Maxim Markevitch, Adam Foster, Randall K. Smith, Michael Loewenstein, and Scott W. Randall. Detection of an unidentified emission line in the stacked x-ray spectrum of galaxy clusters. *The Astrophysical Journal*, 789(1):13, jun 2014.
- [53] A. Boyarsky, O. Ruchayskiy, D. Iakubovskiy, and J. Franse. Unidentified line in x-ray spectra of the andromeda galaxy and perseus galaxy cluster. *Phys. Rev. Lett.*, 113:251301, Dec 2014.
- [54] A. Boyarsky, J. Franse, D. Iakubovskiy, and O. Ruchayskiy. Checking the dark matter origin of a 3.53 keV line with the milky way center. *Phys. Rev. Lett.*, 115:161301, Oct 2015.
- [55] Alexander Merle and Aurel Schneider. Production of sterile neutrino dark matter and the 3.5 keV line. *Physics Letters B*, 749:283–288, 2015.
- [56] A Neronov and D Malyshev. Toward a full test of the ν msm sterile neutrino dark matter model with athena. *Physical Review D*, 93(6):063518, 2016.
- [57] Takehiko Asaka, Holger Bech Nielsen, and Yasutaka Takanishi. Non-thermal leptogenesis from the heavier majorana neutrinos. *Nuclear Physics B*, 647(1-2):252–274, 2002.
- [58] Wilfried Buchmüller, Roberto D Peccei, and Tsutomu Yanagida. Leptogenesis as the origin of matter. *Annu. Rev. Nucl. Part. Sci.*, 55:311–355, 2005.
- [59] Rupam Kalita and Debasish Borah. Constraining a type I seesaw model with A_4 flavor symmetry from neutrino data and leptogenesis. *Phys. Rev. D*, 92(5):055012, 2015.
- [60] Nayana Gautam and Mrinal Kumar Das. Neutrino mass, leptogenesis and sterile neutrino dark matter in inverse seesaw framework. *Int. J. Mod. Phys. A*, 36(21):2150146, 2021.

- [61] Srubabati Goswami, Ananya Mukherjee, Nimmala Narendra, et al. Leptogenesis and $e\nu$ scale sterile neutrino. *Physical Review D*, 105(9):095040, 2022.
- [62] Pritam Das, Mrinal Kumar Das, and Najimuddin Khan. Phenomenological study of neutrino mass, dark matter and baryogenesis within the framework of minimal extended seesaw. *JHEP*, 03:018, 2020.
- [63] Asmaa Abada, Alvaro Hernandez-Cabezudo, and Xabier Marciano. Beta and neutrinoless double beta decays with keV sterile fermions. *Journal of High Energy Physics*, 2019(1):1–33, 2019.
- [64] M.Yu.Khlopov Ya.B.Zeldovich. Study of the neutrino mass in a double beta-decay. *JETP Letters*, 34(3):141145, 1982.
- [65] S. Abe et al. Precision measurement of neutrino oscillation parameters with kamland. *Phys. Rev. Lett.*, 100:221803, Jun 2008.
- [66] M Agostini, AM Bakalyarov, M Balata, I Barabanov, L Baudis, C Bauer, E Bellotti, S Belogurov, Alice Bettini, L Bezrukov, et al. Improved limit on neutrinoless double- β decay of ^{76}Ge from gerda phase ii. *Physical review letters*, 120(13):132503, 2018.
- [67] Max Aker, Konrad Altenmüller, Marius Arenz, Woo-Jeong Baek, John Barrett, Armen Beglarian, Jan Behrens, Anatoly Berlev, Uwe Besserer, Klaus Blaum, et al. First operation of the katrin experiment with tritium. *The European Physical Journal C*, 80(3):1–18, 2020.
- [68] Steffen Hagstotz, Pablo F. de Salas, Stefano Gariazzo, Sergio Pastor, Martina Gerbino, Massimiliano Lattanzi, Sunny Vagnozzi, and Katherine Freese. Bounds on light sterile neutrino mass and mixing from cosmology and laboratory searches. *Physical Review D*, 104(12), 12 2021.
- [69] VV Vien. $3+1$ active–sterile neutrino mixing in b-l model for normal neutrino mass ordering. *The European Physical Journal C*, 81(5):1–11, 2021.
- [70] VV Vien and HN Long. A 4-based model with linear seesaw scheme for lepton mass and mixing. *Physica Scripta*, 98(1):015301, 2022.
- [71] VV Vien. B- l model with a $4 \times 3 \times 4$ symmetry for $3+1$ active-sterile neutrino mixing. *Journal of Physics G: Nuclear and Particle Physics*, 49(8):085001, 2022.
- [72] VV Vien, Hoang Ngoc Long, and AE Cárcamo Hernández. Lepton masses and mixings, and muon anomalous magnetic moment in an extended b- l model with the type-i seesaw mechanism. *Progress of Theoretical and Experimental Physics*, 2022(9):093B11, 2022.

- [73] Nayana Gautam, R. Krishnan, and Mrinal Kumar Das. Effect of Sterile Neutrino on Low-Energy Processes in Minimal Extended Seesaw With $\Delta(96)$ Symmetry and TM1 Mixing. *Front. in Phys.*, 0:417, 2021.
- [74] Pritam Das, Ananya Mukherjee, and Mrinal Kumar Das. Active and sterile neutrino phenomenology with a4 based minimal extended seesaw. *Nuclear Physics B*, 941:755–779, 2019.
- [75] Steven Weinberg. Baryon- and lepton-nonconserving processes. *Phys. Rev. Lett.*, 43:1566–1570, Nov 1979.
- [76] Soumita Pramanick and Amitava Raychaudhuri. Three-higgs-doublet model under a4 symmetry implies alignment. *Journal of High Energy Physics*, 2018(1):1–21, 2018.
- [77] Stephen F. King and Michal Malinský. A4 family symmetry and quark–lepton unification. *Physics Letters B*, 645(4):351–357, 2007.
- [78] Hajime Ishimori, Tatsuo Kobayashi, Hiroshi Ohki, Yusuke Shimizu, Hiroshi Okada, and Morimitsu Tanimoto. Non-abelian discrete symmetries in particle physics. *Progress of Theoretical Physics Supplement*, 183:1–163, 2010.
- [79] He Zhang. Light Sterile Neutrino in the Minimal Extended Seesaw. *Phys. Lett. B*, 714:262–266, 2012.
- [80] J Schechter and José WF Valle. Neutrino decay and spontaneous violation of lepton number. *Physical Review D*, 25(3):774, 1982.
- [81] S. Dev, Desh Raj, Radha Raman Gautam, and Lal Singh. New mixing schemes for (3+1) neutrinos. *Nuclear Physics B*, 941:401–424, 2019.
- [82] Mayengbam Kishan Singh, S. Robertson Singh, and N. Nimai Singh. Active-Sterile Neutrino Masses and Mixings in A₄ Minimal Extended Seesaw Mechanism. *Int. J. Theor. Phys.*, 61(9):228, 2022.
- [83] Fengpeng An, Guangpeng An, Qi An, Vito Antonelli, Eric Baussan, John Beacom, Leonid Bezrukov, Simon Blyth, Riccardo Brugnera, Margherita Buizza Avanzini, et al. Neutrino physics with *juno*. *Journal of Physics G: Nuclear and Particle Physics*, 43(3):030401, 2016.
- [84] Ke Abe, Ke Abe, H Aihara, A Aimi, R Akutsu, C Andreopoulos, I Anghel, LHV Anthony, M Antonova, Y Ashida, et al. Hyper-kamiokande design report. *arXiv preprint arXiv:1805.04163*, 2018.
- [85] Babak Abi, Roberto Acciarri, Mario A Acero, Giorge Adamov, David Adams, Marco Adinolfi, Zubayer Ahmad, Jhanzeb Ahmed, Tyler Alion, S Alonso Monsalve, et al. Deep underground

- neutrino experiment (dune), far detector technical design report, volume ii: Dune physics. *arXiv preprint arXiv:2002.03005*, 2020.
- [86] Michelle J Dolinski, Alan WP Poon, and Werner Rodejohann. Neutrinoless double-beta decay: status and prospects. *Annual Review of Nuclear and Particle Science*, 69:219–251, 2019.
 - [87] Jun Cao, Guo-yuan Huang, Yu-Feng Li, Yifang Wang, Liang-Jian Wen, Zhi-zhong Xing, Zhen-hua Zhao, and Shun Zhou. Towards the meV limit of the effective neutrino mass in neutrinoless double-beta decays. *Chinese Physics C*, 44(3):031001, 2020.
 - [88] André De Gouvêa, Manibrata Sen, Walter Tangarife, and Yue Zhang. Dodelson-widrow mechanism in the presence of self-interacting neutrinos. *Physical review letters*, 124(8):081802, 2020.
 - [89] Sacha Davidson, Enrico Nardi, and Yosef Nir. Leptogenesis. *Physics Reports*, 466(4-5):105–177, 2008.
 - [90] Laura Covi, Esteban Roulet, and Francesco Vissani. CP violating decays in leptogenesis scenarios. *Physics Letters B*, 384(1-4):169–174, 1996.
 - [91] Enrico Nardi, Yosef Nir, Esteban Roulet, and Juan Racker. The importance of flavor in leptogenesis. *Journal of High Energy Physics*, 2006(01):164, 2006.
 - [92] Guy Engelhard, Yuval Grossman, and Yosef Nir. Relating leptogenesis parameters to light neutrino masses. *JHEP*, 07:029, 2007.